Journal of Biomolecular NMR, 3 (1993) 41–54
ESCOM

J-Bio NMR 097

Aliphatic ^{1}H and ^{13}C resonance assignments for the 26-10 antibody V_L domain derived from heteronuclear multidimensional NMR spectroscopy

Keith L. Constantine*, Valentina Goldfarb, Michael Wittekind, Mark S. Friedrichs, James Anthony, Shi-Chung Ng and Luciano Mueller

Bristol-Myers Squibb Pharmaceutical Research Institute, P.O. Box 4000, Princeton, NJ 08543, U.S.A.

Received 20 August 1992
Accepted 6 October 1992

Keywords: Antibody domain; Chemical shift; Side-chain assignments; Triple resonance

SUMMARY

Extensive ^{1}H and ^{13}C assignments have been obtained for the aliphatic resonances of a uniformly ^{13}C- and ^{15}N-labeled recombinant V_L domain from the anti-digoxin antibody 26-10. Four-dimensional triple resonance NMR data acquired with the HNCAHA and HN(CO)CAHA pulse sequences [Kay et al. (1992) *J. Magn. Reson.*, **98**, 443–450] afforded assignments for the backbone H^N, N, H^α and C^α resonances. These data confirm and extend H^N, N and H^α assignments derived previously from three-dimensional ^{1}H-^{15}N NMR studies of uniformly ^{15}N-labeled V_L domain [Constantine et al. (1992), *Biochemistry*, **31**, 5033–5043]. The identified H^α and C^α resonances provided a starting point for assigning the side-chain aliphatic ^{1}H and ^{13}C resonances using three-dimensional HCCH-COSY and HCCH-TOCSY experiments [Clore et al. (1990), *Biochemistry*, **29**, 8172–8184]. The C^α and C^β chemical shifts are correlated with the V_L domain secondary structure. The extensive set of side-chain assignments obtained will allow a detailed comparison to be made between the solution structure of the isolated V_L domain and the X-ray structure of the V_L domain within the 26-10 Fab.

INTRODUCTION

Antibodies against the cardiac glycoside digoxin are used in the treatment of congestive heart failure to measure serum digoxin levels and to counteract the toxic effects of excess digoxin (Smith et al., 1976). X-ray structures for the digoxin complexed and uncomplexed Fab fragment of the anti-digoxin antibody 26-10 have been reported (Jeffrey, P.D., personal communication). The X-ray analysis revealed that the 26-10 Fab conformation changes little upon complexation with digoxin. In addition, the crystallographic results indicate that the high affinity of 26-10 for

*To whom correspondence should be addressed.

digoxin ($K_a = 7 \times 10^9$ M^{-1} for IgG; Anthony et al., 1992) is due primarily to shape complementarity and displacement of water from the combining site. The effects of various residue substitutions and hapten modifications on 26-10/hapten interactions have been characterized (Schildbach et al., 1991), affording extensive affinity data. The 26-10 antibody is therefore an attractive system for detailed biophysical studies.

In concert with the biochemical and crystallographic investigations of the 26-10 antibody, we have undertaken NMR studies of this system (Anthony et al., 1992; Constantine et al., 1992a,b). The long-term goal of this project is to characterize the solution structure and dynamic behavior of native and mutant 26-10 Fv fragments with and without various digoxin congeners bound, and to relate this information to observed specificities and affinities. The 26-10 V_L and V_H domains have been co-expressed in *Escherichia coli*, and the soluble Fv was found to retain high, albeit slightly reduced, digoxin affinity ($K_a = 1.3 \times 10^9$ M^{-1}; Anthony et al., 1992). In addition, the uncomplexed 26-10 Fv was found to be relatively stable, with a greater than 48-hour half-life for domain-domain dissociation at 37 °C. Consistent with these results, a preliminary ^{1}H-NMR analysis indicated a stable, folded conformation for the soluble Fv (Anthony et al., 1992).

During preparation of the 26-10 Fv fragment, it was discovered that the V_L domain is expressed much more efficiently than the V_H domain, and that the V_L domain is soluble at high (~ mM) concentrations (Anthony et al., 1992; Constantine et al., 1992a). This provides an opportunity to assign and characterize the solution structure and dynamics of the isolated V_L domain. Basic questions regarding the conformation and stability of the V_L domain in the absence of quaternary interactions can thus be addressed. Also, assignment of the isolated V_L domain ($M_r \sim 12$ K) is expected to greatly facilitate assignment of the Fv fragment (M_r ~25 K).

We have previously reported assignments for the backbone ^{1}H and ^{15}N resonances for the 26-10 V_L domain on the basis of 3D ^{1}H-^{15}N NMR data acquired with a uniformly ^{15}N-labeled sample (Constantine et al., 1992a). Backbone assignments were obtained for all residues except Ser^{28}, Lys^{55} and Pro^{100}. Limited side-chain ^{1}H assignments were also reported. This study revealed that the isolated V_L domain contains features of secondary structure very similar to those observed crystallographically for the V_L domain within the Fab (Jeffrey, P.D., personal communication). β-Strands A, B, C, C′, C″, D, E, F, and G were all located. The assigned backbone N and H^N resonances served as the basis for a detailed characterization of the V_L domain backbone dynamics via measurements of ^{15}N relaxation parameters and ^{1}H-^{2}H exchange rates (Constantine et al., 1992b). This investigation demonstrated that turns, complementarity determining region (CDR) loops, and parts of the outer β-strands (β-strands A, B and G) have enhanced flexibility relatively to the central framework region. The relaxation data also indicates that the 26-10 V_L domain is predominantly monomeric under our conditions.

In this paper we report assignments for the backbone C^α resonances and extensive side-chain

---

Abbreviations: CDR, complementarity determining region; Fab, antigen-binding fragment; FID, free-induction decay; Fv, antibody fragment composed of the V_H and V_L domains; HCCH-COSY, 3D proton-carbon-proton correlation spectroscopy; HCCH-TOCSY, 3D proton-carbon-proton total correlation spectroscopy; HNCAHA, 4D amide proton-nitrogen-alpha carbon-alpha proton correlation spectroscopy; HN(CO)CAHA, 4D amide proton-nitrogen-alpha carbon (via carbonyl carbon relay)-alpha proton correlation spectroscopy; IgG, immunoglobulin G; pH*, pH meter reading uncorrected for deuterium isotope effects; TSP, (trimethylsilyl)[2,2,3,3,-$^2H_4$]proprionate; V_H, variable domain of the antibody heavy chain; V_L, variable domain of the antibody light chain; 2D, two-dimensional; 3D, three-dimensional; 4D, four-dimensional.

^{1}H and ^{13}C resonance assignments for the 26-10 V_L domain. These assignments are based on data acquired with a uniformly $^{15}N/^{13}C$-labeled V_L domain sample. The C^{α} assignments were derived using two recently developed 4D triple resonance NMR experiments (Kay et al., 1992). These are the HNCAHA experiment, which correlates intraresidue N, H^N, H^{α} and C^{α} resonances, and the HN(CO)CAHA experiment, which correlates the N and H^N resonances of residue i with the C^{α} and H^{α} resonances of residue i−1. C^{α} assignments have been obtained for all residues except Pro^{100} and Gly^{104}. Analysis of the 4D data confirms the backbone assignments previously obtained (Constantine et al., 1992a) for all residues, except for the Asp^{65} H^{α} resonance, which was previously confused with the H^{β} resonance of Ser^{14}. Using the C^{α} and H^{α} assignments as a starting point, side-chain ^{13}C and ^{1}H assignments were derived from an analysis of HCCH-COSY and HCCH-TOCSY spectra (Bax et al., 1990a,b; Clore et al., 1990). Side-chain assignments have been obtained for all residues except Pro^{49} and Pro^{100}. Most aliphatic side chains have been assigned completely. In total, 91% of the side-chain aliphatic ^{1}H resonances have been assigned. Only 48% of these resonances were assigned previously using 3D ^{1}H-^{15}N NMR data (Constantine et al., 1992a). Several corrections to the limited side-chain ^{1}H assignments previously reported are noted.

MATERIALS AND METHODS

Protein isolation and sample preparation

Details on the expression and purification of unlabeled and uniformly ^{15}N-labeled 26-10 V_L domain have been described elsewhere (Anthony et al., 1992; Constantine et al., 1992a). The same procedures were used to produce uniformly $^{15}N/^{13}C$-labeled V_L domain, using the appropriate growth media. One liter of growth media (pH 7.0) contained the following: 10.5 g K_2HPO_4, 2 mg $CaCl_2 \cdot 2\ H_2O$, 2 mg $ZnSO_4 \cdot 7\ H_2O$, 2 mg $MnSO_4$, 4 ml of 1 M $MgSO_4$, 1.08 mg $FeCl_3 \cdot 6\ H_2O$, 70 μg $MoO_4 \cdot H_2O$, 80 μg $CuSO_4$, 20 μg H_3BO_3, 20 mg thiamine, 5 mg niacin, 60 μg biotin, 100 mg ampicillin, 1 g ^{15}N-ammonium sulfate (Isotec Inc.), and 2 g ^{13}C-glucose (Isotec Inc.).

The $^{15}N/^{13}C$-labeled V_L sample was concentrated to ~ 3.0 mM in 0.5 ml of buffer containing 50 mM deuterated NaOAc, 0.001% NaN_3 in 90%/10% (v/v) $H_2O/^{2}H_2O$, pH 5.5. After acquisition of the 4D HNCAHA and HN(CO)CAHA spectra, the sample was lyophilized to a dry powder, redissolved in 99.9% $^{2}H_2O$, lyophilized a second time, and redissolved in 99.96% $^{2}H_2O$, pH* 5.5 prior to collection of the 3D HCCH-COSY and HCCH-TOCSY data.

NMR data acquisition and processing

NMR experiments were recorded at 30 °C using a Varian UNITY-600 spectrometer operating at 599.95, 150.87 and 60.80 MHz for ^{1}H, ^{13}C and ^{15}N, respectively. All spectra were acquired using a ^{1}H-^{13}C-^{15}N triple resonance probe, and an external frequency synthesizer was used to provide a fourth channel for carbonyl decoupling. The ^{1}H carrier frequency was placed on the H_2O (or residual $^{2}H_2O$) resonance, which is at 4.76 ppm relative to an external TSP standard. Solvent suppression was achieved by low-power irradiation during the recycle delay (1.2–1.3 s). The ^{13}C and ^{15}N chemical shifts were referenced indirectly to TSP and NH_3, respectively, using methods detailed elsewhere (Fairbrother et al., 1992). All NMR spectra were processed on Silicon Graphics workstations using a modified version of the FELIX program (Hare Research, Inc.).

The 4D HNCAHA and HN(CO)CAHA spectra were recorded with published pulse sequences

and phase cycling schemes (Kay et al., 1992), using shared constant-time evolution in t_1 and t_2. Carrier frequencies for the heteronuclei were set to 120.0 ppm for ^{15}N, 57.9 ppm for ^{13}C (C^{α}), and 177 ppm for ^{13}C (CO). Spectral widths of 8000 Hz, 2000 Hz, 3000 Hz and 3000 Hz were used for F_4 (H^N), F_3 (N), F_2 (H^{α}), and F_1 (C^{α}), respectively. During processing (see below), the upfield half of the acquisition dimension was discarded, yielding a spectral width of 4000 Hz in F_4. Quadrature detection in t_1, t_2 and t_3 was achieved using the States-TPPI method (Marion et al., 1989b). The data were collected as 8 complex (F_1) by 8 complex (F_2) by 16 complex (F_3) by 416 complex (F_4) data points, yielding acquisition times of 2.7 ms in F_1 and F_2, 8.0 ms in F_3, and 52 ms in F4. Each FID consisted of 32 signal-averaged transients. ^{15}N decoupling during ^1H acquisition was achieved using the WALTZ-16 sequence (Shaka et al., 1983). For the HNCAHA experiment, the SEDUCE-1 sequence (McCoy and Mueller, 1992) was used to decouple carbonyls. Optimized values for all delays and radiofrequency field strengths (Kay et al., 1992) were used.

The HNCAHA and HN(CO)CAHA data were transformed into 64 (F_1) by 64 (F_2) by 64 (F_3) by 128 (F_4) real point data matrices. Prior to transformation, the F_4 data were truncated at 32 ms, the F_1 and F_2 data were extended from 8 to 24 data points by mirror-image linear prediction (Zhu

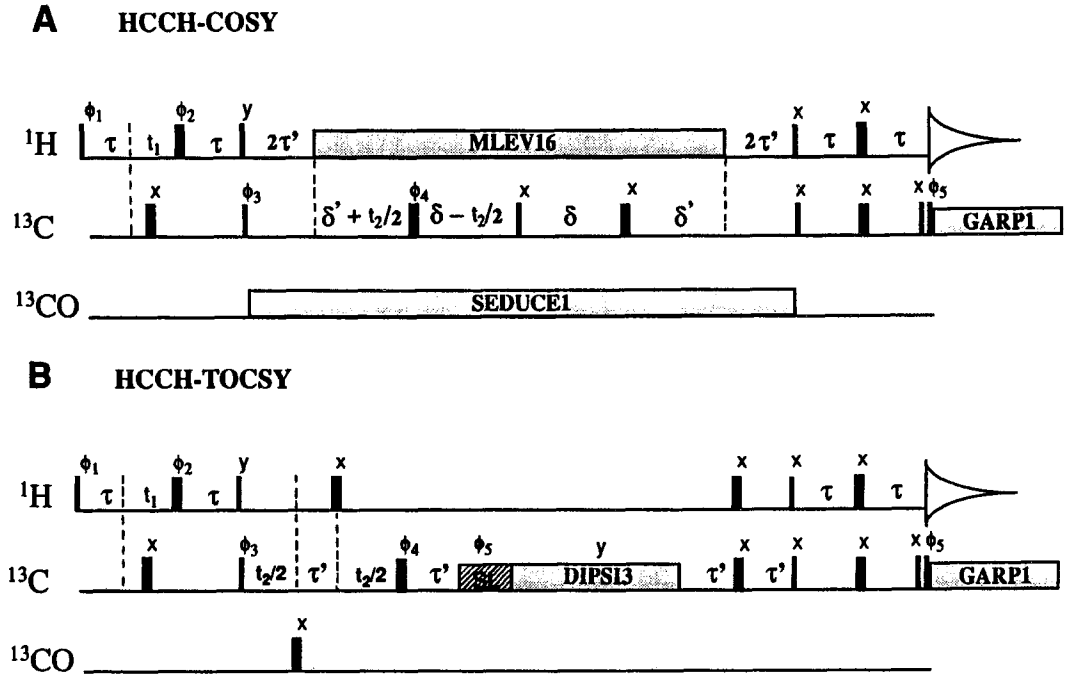

Fig. 1. Pulse schemes for the modified (A) HCCH-COSY and (B) HCCH-TOCSY experiments. Thin vertical bars indicate 90° pulses, and thick vertical bars indicate 180° pulses. The delays τ, τ' and δ were set to 1.6 ms, 1.1 ms and 4.0 ms, respectively, and $\delta' = \delta - 2\tau'$. The spin-lock trim pulse (SL) in the HCCH-TOCSY was applied for 1.0 ms. The first and last ^{13}C 180° pulses of both sequences were composite $90_x180_y90_x$ pulses. A selective hermite 180° pulse was applied to ^{13}CO in the HCCH-TOCSY, and ^{13}CO decoupling was achieved by using SEDUCE-1 (McCoy and Mueller, 1992) in the HCCH-COSY. The phase cycling used for both experiments is as follows: $\varphi_1 = x$; $\varphi_2 = x,y$; $\varphi_3 = x$; $\varphi_4 = 2(x),2(y),2(-x),2(-y)$; $\varphi_5 = 4(x), 4(-x)$; receiver = (x), 2(−x),(x). Quadrature detection in t_1 and t_2 was obtained by hypercomplex cycling (Mueller and Ernst, 1979; States et al., 1982) of φ_1 and φ_3, respectively.

and Bax, 1990), and low-frequency deconvolution (Marion et al., 1989a) was applied to the acquisition dimension to remove the residual H_2O signal. The time domain data were multiplied by a 70°-shifted skewed sine-bell weighting function in F_4 and by a cosine-bell weighting function in F_1, F_2 and F_3. The F_1, F_2 and F_3 data were zero-filled before Fourier transformation. All data upfield of the H_2O resonance in F_4 (H^N) were discarded, and the F_2 (H^α) data were adjusted such that the final sweep width in this dimension was 2000 Hz centered at 4.49 ppm.

HCCH-COSY and HCCH-TOCSY spectra were recorded using modified versions of published pulse sequences (Bax et al., 1990a,b; Clore et al., 1990), as detailed in Fig. 1. Both sequences incorporate an eight-step phase cycle per FID (8 signal-averaged transients). The HCCH-COSY was modified to include ^1H and CO decoupling during ^{13}C t_2 evolution, which was recorded in a constant-time mode. Carrier frequencies for ^{13}C were set to 41.2 ppm (aliphatic) and 177 ppm (CO). Spectral widths of 8000 Hz, 4000 Hz and 8000 Hz were used in F_1 (^1H), F_2 (^{13}C aliphatic) and F_3 (^1H), respectively. Quadrature detection in t_1 and t_2 was achieved by hypercomplex data acquisition (Mueller and Ernst, 1979; States et al., 1982). The data were collected as 128 complex (F_1) by 32 complex (F_2) by 512 complex (F_3) data points, yielding acquisition times of 16 ms in F_1, 8 ms in F_2, and 64 ms in F_3. A mixing time of 23 ms was used during the DIPSI-3 isotropic mixing sequence (Shaka et al., 1988) of the HCCH-TOCSY.

The HCCH-TOCSY and HCCH-COSY data were transformed into 256 (F_1) by 64 (F_2) by 256 (F_3) real data point matrices. The first complex t_2 data point was replaced by a back-predicted point, and the t_2 data were extended forward 16 points, by complex linear prediction. The time domain data were multiplied by cosine-bell, 70°-shifted sine-bell and 70 °-shifted skewed sine-bell weighting functions in F_1, F_2 and F_3, respectively, prior to Fourier transformation. The frequency domain F_1 and F_3 data were adjusted such that the final sweep widths in these dimensions were 4000 Hz centered at 2.89 ppm.

RESULTS AND DISCUSSION

Backbone N, H^N, C^α and H^α assignments

Since it is predominantly a β-sheet protein with relatively good chemical shift dispersion, the assignment of the backbone N, H^N and H^α resonances of the 26-10 V_L domain was reasonably straightforward using 3D ^{15}N-edited NMR experiments (Constantine et al., 1992a). Side-chain assignments proved considerably more difficult to obtain from these data. For a protein the size of the 26-10 V_L domain (~ 12 K), ^1H side-chain assignments without the benefit of ^{13}C-editing may prove insufficient for assigning NOESY cross peaks. The availability of uniformly $^{15}N/^{13}C$-labeled V_L domain made extensive ^{13}C and ^1H assignments possible. The first step in this analysis is to confirm and extend the previously obtained N, H^N and H^α assignments, and to assign the C^α resonances. A variety of 3D triple resonance experiments have been developed which could accomplish this task (Kay et al., 1990; Powers et al., 1992). We opted to use two recently developed 4D triple resonance pulse sequences – the HNCAHA and HN(CO)CAHA experiments (Kay et al., 1992) – which together afford a powerful approach for assigning backbone N, H^N, H^α and C^α resonances. These spectra are also expected to yield readily to automated analysis.

The assignment strategy is illustrated in Fig. 2 for Ser^{57}, Val^{56} and Lys^{55}. Figure 2A shows the intraresidue cross peak for Ser^{57} in the HNCAHA spectrum. The F_4,F_3 plane is plotted, with F_1 and F_2 fixed at the Ser^{57} C^α and H^α frequencies, respectively. The Ser^{57} N and H^N frequencies are

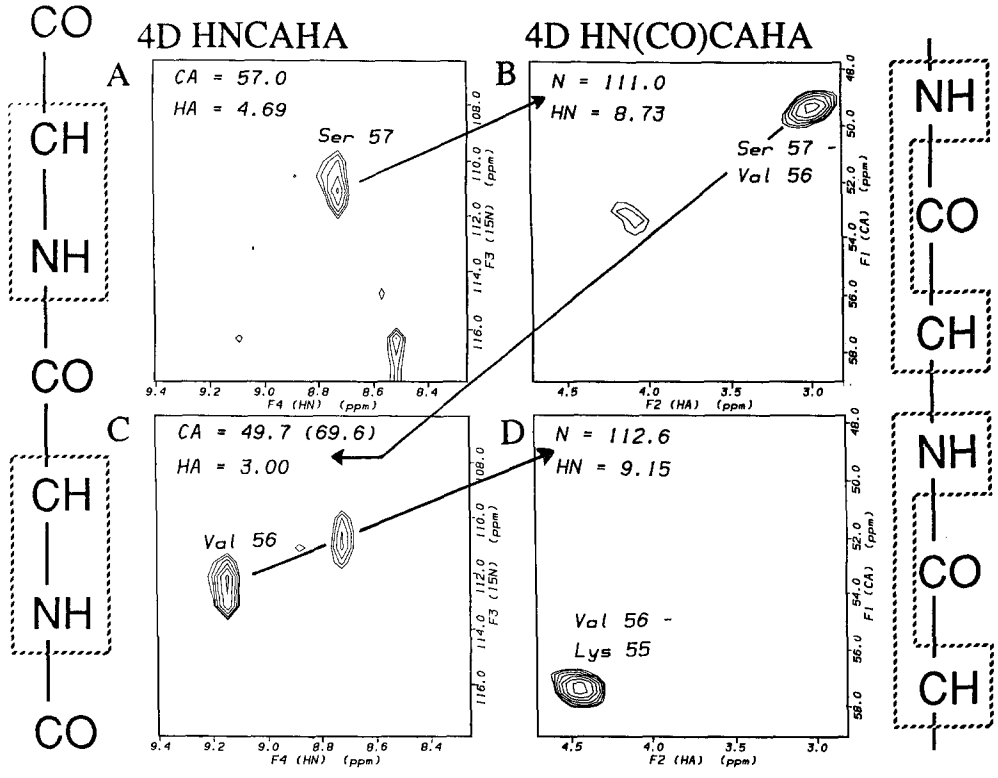

Fig. 2. 600 MHz 4D HNCAHA and HN(CO)CAHA spectra of the 26-10 V_L domain: expanded planes illustrating assignment of the backbone resonances of Ser^{57}, Val^{56}, and Lys^{55}. (A) F_3,F_4 plane (F_1,F_2 fixed) of the HNCAHA spectrum containing the Ser^{57} intraresidue cross peak. (B) F_1,F_2 plane (F_3,F_4 fixed) of the HN(CO)CAHA spectrum containing the Ser^{57} (N, H^N) → Val^{56} (C^α, H^α) interresidue cross peak. The Val^{56} C^α resonance is folded from its true location at 69.9 ppm. (C) HNCAHA F_3,F_4 plane containing the Val^{56} intraresidue cross peak. (D) HN(CO)CAHA F_1,F_2 plane containing the Val^{56} (N, H^N) → Lys^{55} (C^α, H^α) interresidue cross peak. The connectivities are illustrated by the boxed regions on the schematic polypeptide backbones adjacent to each panel. The spectra were recorded at 30°C on a ~ 3.0 mM uniformly $^{15}N/^{13}C$-labeled V_L sample dissolved in 90%/10% (v/v) $H_2O/^2H_2O$ containing 50 mM deuterated NaOAc, 0.001% NaN_3, pH 5.5.

fixed in a plot of the F_1,F_2 plane of the HN(CO)CAHA spectrum (Fig. 2B). An interresidue cross peak connecting the Ser^{57} N and H^N resonances with the Val^{56} C^α and H^α resonances is present in this panel. The Val^{56} C^α and H^α chemical shifts are fixed for the next F_3,F_4 plot of the HNCAHA spectrum (Fig. 2C), which contains the Val^{56} intraresidue cross peak. Note that this panel also contains a weaker interresidue cross peak to Ser^{57}. The Val^{56} N and H^N chemical shifts define the next F_1,F_2 plot of the HN(CO)CAHA spectrum (Fig. 2D), which contains a cross peak locating the C^α and H^α resonances of Lys^{55}. In our previous study (Constantine et al., 1992a), Lys^{55} was completely unassigned, since its backbone N/H^N correlation could not be located. The C^α = 57.4 ppm, H^α = 4.44 ppm plane of the HNCAHA spectrum (not shown) contains relatively weak cross peaks at N = 110.4 ppm, H^N = 7.56 ppm and at N = 130.7 ppm, H^N = 8.10 ppm. Sequential connectivities from either of these N/H^N correlations to Tyr^{54} C^α/H^α have not been located. Thus, unambiguous assignments have still not been obtained for the Lys^{55} N and H^N resonances. Since

the N, H^N and H^α assignments of Tyr^{54} were already known, the sequential walk through the 4D data was resumed at this residue. In general, one works backwards through the sequence until a Pro, Gly or ambiguity is encountered. Since we are mostly concerned with confirming established backbone assignments (Constantine et al., 1992a), cases of C^α/H^α degeneracy did not present a problem. We note that recently developed 3D triple resonance experiments which yield correlations to C^β (Grzesiek and Bax, 1992; unpublished results) provide a powerful approach for overcoming C^α/H^α degeneracy in de novo assignments.

Analysis of the HNCAHA and HN(CO)CAHA data yielded C^α assignments for all residues except Pro^{100} and several of the Gly residues. Pro^{100} is followed by Pro^{101}; therefore, Pro^{100} does not manifest scalar connectivities to either adjacent residue. Correlations for the Gly residues are often weak or absent due to the influence ^1H-^{13}C coupling during the constant-time F_1,F_2 evolution period (Kay et al., 1992). Since the H^α and $H^{\alpha'}$ resonance positions were previously established for most Gly residues (Constantine et al., 1992a), it was straightforward to locate the ^{13}C planes containing the symmetric $H^\alpha/H^{\alpha'}$ cross peaks in the 3D HCCH-TOCSY and HCCH-COSY data. An example is shown in Fig. 3, which displays an expansion of the ^{13}C = 44.5 ppm

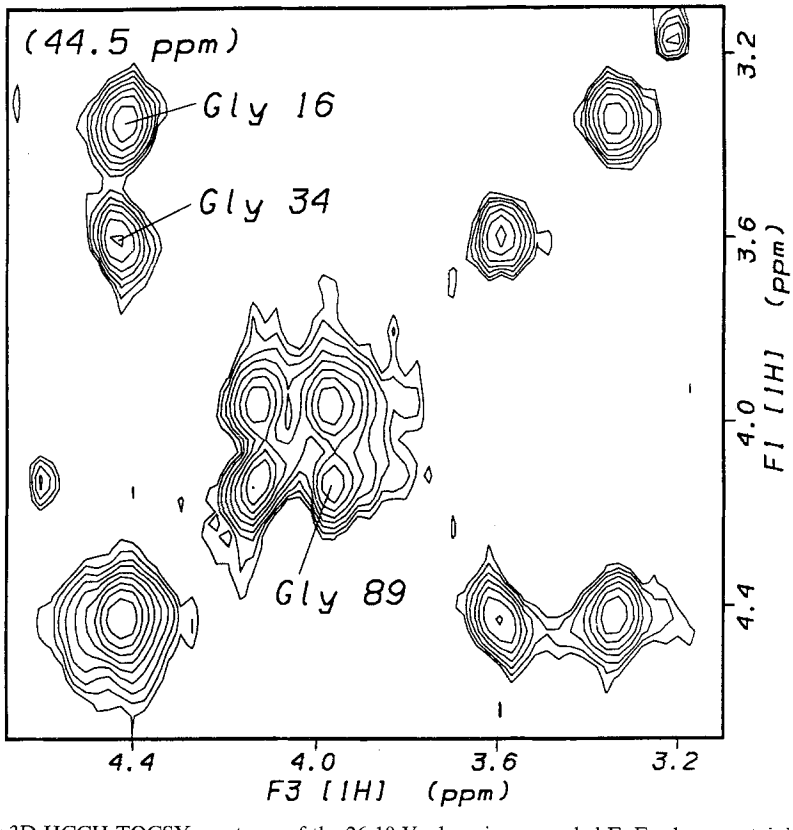

Fig. 3. 600-MHz 3D HCCH-TOCSY spectrum of the 26-10 V_L domain: expanded F_1,F_3 plane containing connectivities involving Gly^{16}, Gly^{34} and Gly^{89}. The $H^\alpha/H^{\alpha\prime}$ cross peaks are labeled, and the chemical shift of the ^{13}C plane (F_2) is given in parentheses. The spectrum was recorded at 30 °C on a ~3.0 mM uniformly $^{15}N/^{13}C$-labeled V_L sample dissolved in 99.96% ^2H_2O containing 50 mM deuterated NaOAc, 0.001% NaN_3, pH* 5.5.

plane of the HCCH-TOCSY spectrum containing $H^{\alpha}/H^{\alpha'}$ cross peaks for Gly^{16}, Gly^{34} and Gly^{89}. Lack of additional correlations, as well as the upfield location of Gly C^{α} resonances relative to other residues, affords unambiguous identifications for the Gly residues. In this manner, C^{α} assignments were established for all Gly residues except Gly^{104}, for which the $H^{\alpha'}$ resonance is either broadened beyond detection or degenerated with the H^{α} resonance at 4.42 ppm.

The backbone assignments obtained by this analysis generally agree with the N, H^{N} and H^{α} assignments reported previously (Constantine et al., 1992a). The only major exception is the H^{α} resonance of Asp^{65}. The N/H^{N} correlations of Asp^{65} and Ser^{14} overlap nearly completely; this resulted in exchange of the assignments of the Asp^{65} H^{α} resonance (4.19 ppm) and the Ser^{14} $H^{\beta 1}$ resonance (3.87 ppm). The conclusions of the previous study are not affected. Also, small ^{15}N chemical shift changes (~ 0.5 to 0.7 ppm) occur for the backbone ^{15}N resonances of Thr^{5} and Thr^{96}. These may be due to slight pH differences among the ^{15}N-labeled and $^{15}N/^{13}C$-labeled samples, or they may result in part from the coarse ^{15}N digital resolution (0.51 ppm/point) used in the present study. All backbone resonance assignments are available as supplementary material from the authors.

Side-chain assignments

The backbone C^{α} and H^{α} assignments derived from the HNCAHA and HN(CO)CAHA spectra served as the starting point for assigning the side-chain aliphatic ^{1}H and ^{13}C resonances via the HCCH-COSY and HCCH-TOCSY spectra. In general, the analysis was accomplished by initally plotting the HCCH-COSY ^{13}C plane containing the C^{α} resonance of interest, taking into account folding of the C^{α} resonance, if necessary. This plane contains the H^{α} F_1,F_3 diagonal peak, as well as cross peaks at $F_1 = H^{\alpha}$, $F_3 = H^{\beta}$. The location of the C^{β} plane was then determined by examining a 1D vector at the symmetric $F_1 = H^{\beta}$, $F_3 = H^{\alpha}$ position. This vector passes through the symmetric H^{β}/H^{α} cross peak in the C^{β} plane. The C^{β} plane was then plotted and, in the cases of longer side-chains, connectivities further along the side-chain were traced in an analogous manner. The HCCH-TOCSY spectrum was analyzed in concert with the HCCH-COSY spectrum. In addition to H^{α}/H^{β} connectivities, C^{α} planes in the HCCH-TOCSY contain cross peaks to additional side-chain protons at $F_1 = H^{\alpha}$, F_3 = side-chain ^{1}H. The planes of the side-chain ^{13}C resonances were located by plotting vectors at the symmetric F_1 = side-chain ^{1}H, $F_3 = H^{\alpha}$ position. Quite often, simply determining the chemical shift of a side-chain ^{13}C resonance makes identification possible, as the ^{13}C resonances tend to fall into non-overlapping ranges for specific atom types (Clore et al., 1990). Exceptions include the C^{β} and C^{γ} resonances of Arg, Glu, Gln and Met residues, and the C^{β} and C^{δ} resonances of Lys residues. All side-chain assignments were verified by examination of various ^{13}C planes in both the HCCH-COSY and HCCH-TOCSY spectra.

The short side chains (Ala, Thr and residues containing AMX ^{1}H spin systems) were, in general, readily assigned from inspection of the data. Several of the sixteen Ser residues proved difficult to assign completely, either due to weakness of the side-chain resonances (e.g. Ser^{26} and Ser^{48}) or due to overlap with other spin systems (e.g. Ser^{68}). Nearly all assignments for the short side-chains obtained here agree with the limited assignments reported previously (Constantine et al., 1992a). The exceptions are the H^{β} resonance of Ser^{14} (which, as discussed above, was previously confused with the Asp^{65} H^{α} resonance) and the H^{β} and $H^{\beta'}$ resonances of Cys^{93} at 2.27 and 1.40 ppm, respectively. These latter resonances, particularly $H^{\beta'}$, are at highly upfield-shifted positions.

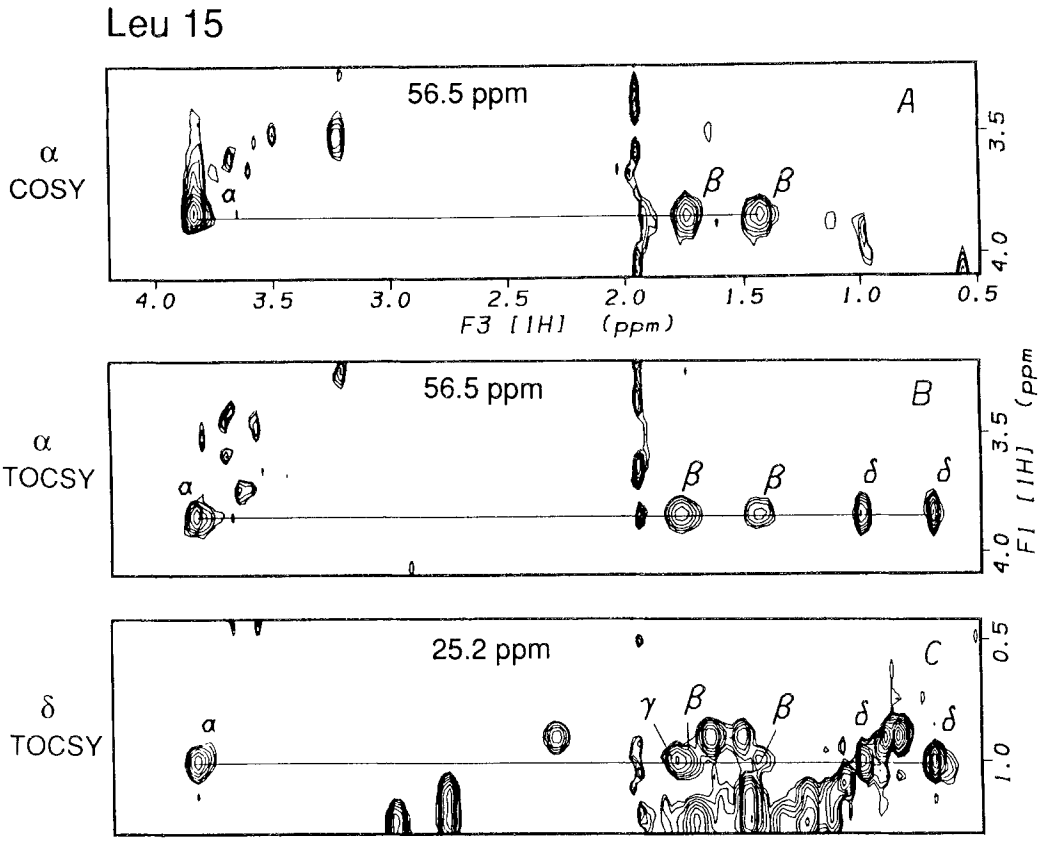

Fig. 4. 600-MHz 3D HCCH-COSY and HCCH-TOCSY spectra of the 26-10 V_L domain: expanded F_1,F_3 planes illustrating the assignment of the Leu[15] side-chain. (A) C^{α} plane of the HCCH-COSY spectrum showing H^{α}/H^{β} connectivities. (B) C^{α} plane of the HCCH-TOCSY spectrum showing H^{α}/side-chain ^1H connectivities. (C) C^{δ} plane of the HCCH-TOCSY spectrum showing H_3^{δ}/H^{α} and H_3^{δ}/side-chain connectivities. Experimental conditions are the same as for Fig. 3.

Longer-branched side-chains containing methyl groups were also relatively easy to assign. This is due to good chemical shift dispersion in both ^1H and ^{13}C, and to the relatively high intensity of cross peaks involving methyl groups. The 26-10 V_L domain contains eleven Leu, five Ile and eight Val residues, most of which have been completely assigned. An example is shown in Fig. 4, which illustrates assignments for the side-chain of Leu[15]. Fig. 4A shows the HCCH-COSY C^{α} plane of Leu[15], which contains H^{α}/H^{β} and $H^{\alpha}/H^{\beta'}$ connectivities. The corresponding plane of the HCCH-TOCSY is shown in Fig. 4B, which contains in addition H^{α}/H^{δ} and $H^{\alpha}/H^{\delta'}$ cross peaks. Figure 4C shows the C^{δ} plane of Leu[15]. Note that the H^{β} and H^{γ} resonances overlap. This was resolved by observation of H^{δ}/H^{γ} and $H^{\delta'}/H^{\gamma}$ correlations in the HCCH-COSY spectrum (not shown). All branched side-chain assignments were obtained in a similar fashion. The only correction to the limited branched side-chain assignments reported previously is for the Val[56] $H^{\delta'}$, which is at 1.04 ppm rather than 0.20 ppm.

The longer unbranched side-chains – Arg, Gln, Glu, Lys, Met and Pro – are somewhat more difficult to assign due to ^1H and ^{13}C chemical shift degeneracy among certain side-chain groups

(Fairbrother et al., 1992). Nevertheless, the resolving power of the HCCH-COSY and HCCH-TOCSY spectra is such that extensive, often complete, side-chain assignments have been obtained for most of these residues. An example is shown in Fig. 5, which illustrates assignments for the side-chains of Pro^{12}. Figures 5A and B show the Pro^{12} C^{α} planes in the HCCH-COSY and HCCH-TOCSY spectra, respectively. The assignments indicated in Figs. 5A and B are confirmed in Fig. 5C, which shows the Pro^{12} C^{δ} plane of the HCCH-TOCSY spectrum. Residues in the long unbranched side-chain class for which extensive side-chain assignments have not yet been obtained are Glu^{43}, Pro^{49}, Pro^{100} and Pro^{101}. All side-chain assignments, including corrections for the side-chain ^1H resonances of Glu^{27}, Arg^{66} and Lys^{112}, are available as supplementary material from the authors.

Correlations of C^{α} and C^{β} chemical shifts with secondary structure

Recently, correlations have been observed between C^{α} (Spera and Bax, 1991; Wishart et al., 1991; Fairbrother et al., 1992) and C^{β} (Spera and Bax, 1991) chemical shifts and the local backbone conformations for a number of proteins with known X-ray structures. These correla-

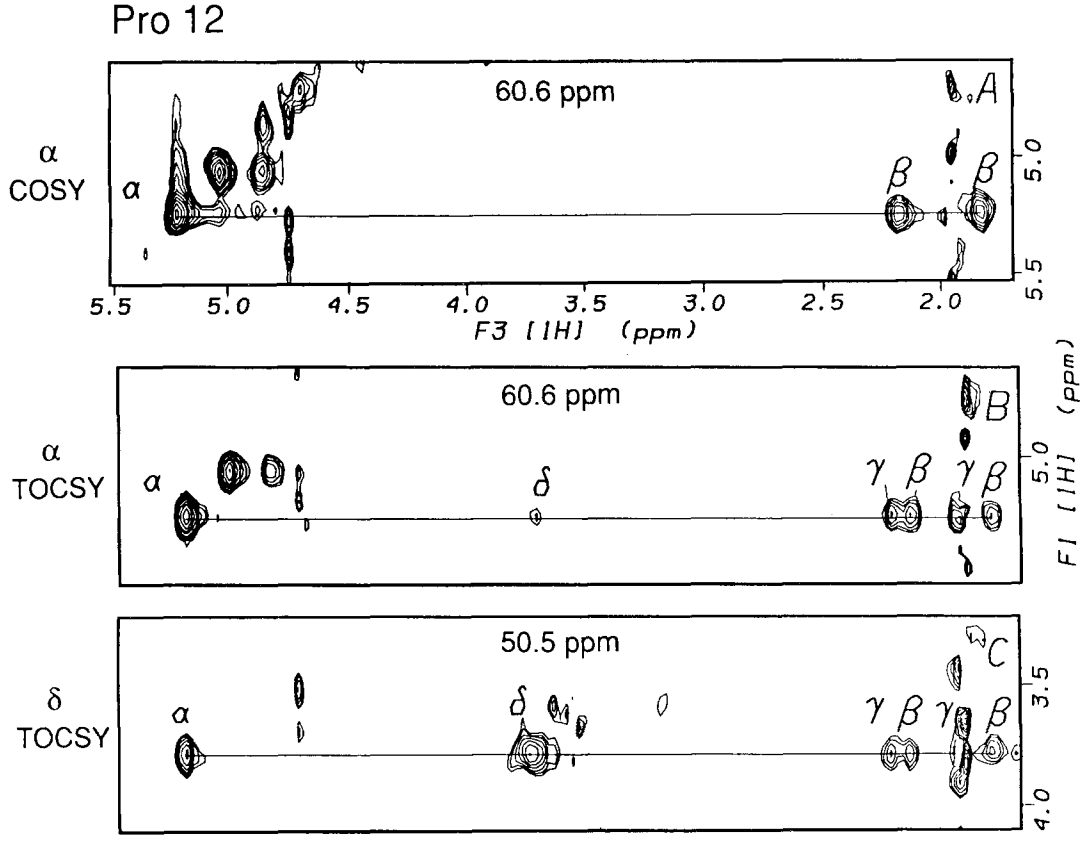

Fig. 5. 600-MHz 3D HCCH-COSY and HCCH-TOCSY spectra of the 26-10 V_L domain: expanded F_1,F_3 planes illustrating the assignment of the Pro^{12} side-chain. (A) C^{α} plane of the HCCH-COSY spectrum showing H^{α}/H^{α} connectivities. (B) C^{α} plane of the HCCH-TOCSY spectrum showing H^{α}/side-chain ^1H connectivities. (C) C^{δ} plane of the HCCH-TOCSY spectrum showing H^{δ}/H^{α} and H^{δ}/side-chain ^1H connectivities. Experimental conditions are the same as for Fig. 3.

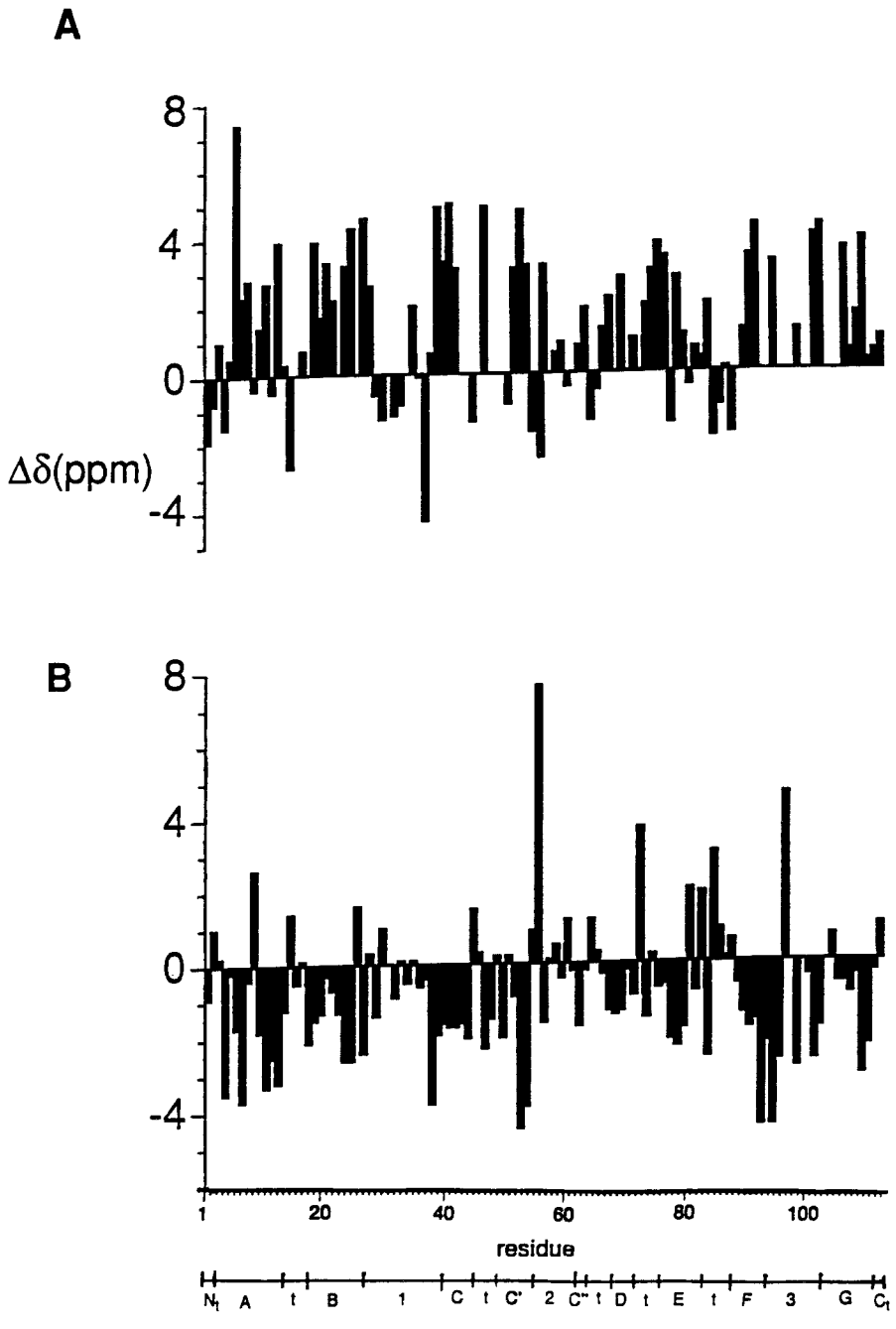

Fig. 6. Histograms showing Δ δ, the measured ^{13}C chemical shift minus the 'random coil' ^{13}C chemical shifts (Spera and Bax, 1991), for (A) the C^{β} and (B) the C^{α} resonances of the 26-10 V_L domain. Cys residues were not included in (A), and His residues were excluded from both (A) and (B). A Δ δ value of 0 was assigned for residues without C^{α} or C^{β} assignments. Residue numbers are displayed along the lower horizontal axis. At the bottom of the diagram, regions of the sequence corresponding to the N-terminus (N_t), the C-terminus (C_t), turns(t), CDRs (numbers) and β-strands (capital letters) are indicated.

tions have also been observed in a protein for which the elements of secondary structure have been characterized exclusively by solution NMR methods (Wittekind et al., 1992). Relative to random coil positions (Spera and Bax, 1991), C^{α} resonances tend to shift upfield in β-sheets and extended strands, and they tend to shift downfield in helices. The opposite trends hold for the C^{β} resonances. Figure 6 displays the secondary shifts (deviations from random coil values) for the C^{β} (Fig. 6A) and the C^{α} (Fig. 6B) resonances of the 26-10 V_L domain. The sequence numbering and backbone conformations are indicated along the bottom of the figure. Overall, the C^{α} and C^{β} shifts of the 26-10 V_L domain show the obvious signature of a protein composed primarily of β-sheets, with the C^{α} resonances displaying predominantly negative secondary shifts and the C^{β} resonances displaying predominantly positive secondary shifts. These regions correlate well with the known locations of the β-strands (Constantine et al., 1992a; Jeffrey, P.D., personal communication). Most of the exceptions to the expected trends can be related to known perturbations of the regular secondary structure. For example, β-strand A is interrupted by a *cis*-Pro residue at position 8. The following residue, Leu^9, adopts φ and ψ angles of −73° and −52°, respectively, in the 2.5–Å resolution X-ray structure of the digoxin-complexed 26-10 Fab (Jeffrey, P.D., personal communication), disrupting β-strand A. Similarly, deviations in β-strands C′ and G are accounted for by bulge features (Chothia et al., 1985) involving residues Leu^{51} through Ile^{53} and Gly^{104} through Gly^{106}, respectively. On the other hand, exceptions involving Val^2 through Met^4 cannot be explained on the basis of the X-ray structure, as these residues all adopt φ and ψ angles consistent with a β-sheet conformation. NOE information also indicates that these residues adopt, at least on average, an extended conformation (Constantine et al., 1992a). However, these residues have been shown to be flexible by ^{15}N-relaxation data and ^{1}H-^{2}H exchange rates (Constantine et al., 1992b). This may account for their uncharacteristic C^{α} and C^{β} chemical shifts. Finally, we note that Val^{56} displays an unusually large positive secondary shift of 7.6 ppm for its C^{α} resonance. In the X-ray structure of the digoxin-complexed 26-10 Fab (Jeffrey, P.D., personal communication), this residue has a φ angle of +39° and a ψ angle of −40°. Therefore, it appears to adopt an unusual conformation, consistent with the large secondary shift observed.

CONCLUDING REMARKS

We have obtained at least partial assignments for 112 of the 113 26-10 V_L residues, and complete ^{1}H and ^{13}C assignments have been reported for most of the aliphatic portions of the side-chains. The only remaining residue for which no assignments have yet been obtained is Pro^{100}, which is a difficult case, since it is followed by another Pro residue (Pro^{101}). Also, only very limited assignments have been obtained for Gln^{43}, Pro^{49} and Pro^{101}. All the side-chain assignments reported here are based on a 'manual' analysis of the NMR data without reference to the X-ray structure (Jeffrey, P.D., personal communication). The remaining ambiguities may be cleared up by using an automated assignment protocol based on a general purpose NMR database (under development), and by comparison of NOE and X-ray data. The C^{α} and C^{β} chemical shifts correlate well with secondary structure features observed for the V_L in solution (Constantine et al., 1992a) and for the V_L within the Fab (Jeffrey, P.D., personal communication), further supporting the observed structural integrity of this isolated domain.

The extensive set of assignments reported here will serve as the basis for a detailed characterization of the 26-10 V_L domain solution structure using ^{13}C- and ^{15}N-edited NOESY data. The

results of these efforts will be reported in due course. In addition, many assignments will probably be similar for the V_L domain within the Fv. By reconstituting the Fv from separately expressed V_L and V_H domains, it should be possible to produce Fv samples with only one domain labeled, further enhancing the prospects for obtaining extensive assignments. Efforts along these lines are currently underway. So far, only limited NMR assignments have been reported for Fv fragments (Wright et al., 1990; McManus and Riechman, 1991; Takahashi et al., 1991, 1992), attesting to the difficulty of assigning proteins in the $M_r \sim 25$ K range.

In addition to aiding in the assignment of the 26-10 Fv, many of the 26-10 V_L assignments should assist study of the V_L domains of other antibodies. For example, three crystallographically characterized antibodies display both high V_L domain sequence homology and high conformational similarity to the 26-10 V_L domain (Jeffrey, P.D., personal communication). These are the anti-fluorescein antibody 4-4-20 (Herron et al., 1989), the anti-progesterone antibody DB3 (Arevalo, J.H., unpublished results) and the anti-DNA antibody BV04-01 (Herron et al., 1991), which have 92%, 87% and 94% V_L domain sequence identity with 26-10, respectively. These examples indicate that the 26-10 V_L assignments reported here will prove helpful to other investigators conducting NMR studies of antibody fragments.

ACKNOWLEDGEMENTS

We thank Dr. P.D. Jeffrey and Dr. S. Sheriff for sharing information and insights regarding the structure and function of the 26-10 antibody.

REFERENCES

Anthony, J., Near, R., Wong, S., Iida, E., Ernst, E., Wittekind, M., Haber, E. and Ng, S.-C. (1992) *Mol. Immunol.*, **29**, 1237–1247.

Bax, A., Clore, G.M., Driscoll, P.C., Gronenborn, A.M., Ikura, M. and Kay, L.E. (1990a) *J. Magn. Reson.*, **87**, 620–627.

Bax, A., Clore, G.M. and Gronenborn, A.M. (1990b) *J. Magn. Reson.*, **88**, 425–431.

Chothia, C., Novotny, J., Bruccoleri, R. and Karplus, M. (1985) *J. Mol. Biol.*, **186**, 651–663.

Clore, G.M., Bax, A., Driscoll, P.C., Wingfield, P.T. and Gronenborn, A.M. (1990) *Biochemistry*, **29**, 8172–8184.

Constantine, K.L., Goldfarb, V., Wittekind, M., Anthony, J., Ng, S.-C. and Mueller, L. (1992a) *Biochemistry*, **31**, 5033–5043.

Constantine, K.L., Friedrichs, M.S., Goldfarb, V., Jeffrey, P.D., Sheriff, S. and Mueller, L. (1992b) *Proteins Struct. Funct. Genet.*, in press.

Fairbrother, W.J., Palmer, A.G., Rance, M., Reizer, J., Saier, Jr., M.H. and Wright, P.E. (1992) *Biochemistry*, **31**, 4413–4425.

Grzesiek, S. and Bax, A. (1992) *J. Magn. Reson.*, **99**, 201–207.

Herron, J.N., He, X.M., Mason, M.L., Voss, Jr., E.W. and Edmundson, A.B. (1989) *Proteins Struct. Funct. Genet.*, **5**, 271–280.

Herron, J.N., He, X.M., Ballard, D.W., Blier, P.R., Pace, P.E., Bothwell, A.L.M., Voss, Jr., E.W. and Edmundson, A.B. (1991) *Proteins Struct. Funct. Genet.*, **11**, 159–175.

Kay, L.E., Ikura, M., Tschudin, R. and Bax, A. (1990) *J. Magn. Reson.*, **89**, 496–514.

Kay, L.E., Wittekind, M., McCoy, M.A., Friedrichs, M.S. and Mueller, L. (1992) *J. Magn. Reson.*, **98**, 443–450.

Marion, D., Ikura, M. and Bax, A. (1989a) *J. Magn. Reson.*, **84**, 425–428.

Marion, D., Ikura, M., Tschudin, R. and Bax, A. (1989b) *J. Magn. Reson.*, **85**, 393–399.

McCoy, M.A. and Mueller, L. (1992) *J. Am. Chem. Soc.*, **114**, 2108.

McManus, S. and Riechman, L. (1991) *Biochemistry*, **30**, 5851–5857.

Mueller, L. and Ernst, R.R. (1979) *Mol. Phys.*, **38**, 963–992.

Powers, R., Garrett, D.S., March, C.J., Frieden, E.A., Gronenborn, A.M. and Clore, G.M. (1992) *Biochemistry*, **31**, 4334–4346.

Schildbach, J.F., Panka, D.J., Parks, D.R., Jager, G.C., Herzenberg, L.A., Mudgett-Hunter, M., Haber, E. and Margolies, M.N. (1991) *J. Biol. Chem.*, **266**, 4640–4647.

Shaka, A.J., Keeler, J., Frenkiel, T. and Freeman, R. (1983) *J. Magn. Reson.*, **52**, 355.

Shaka, A.J., Lee, C.J. and Pines, A. (1988) *J. Magn. Reson.*, **77**, 274–293.

Smith, T.W., Haber, E., Yeatman, L. and Butler, Jr., V.P. (1976) *N. Engl. J. Med.*, **294**, 8797.

Spera, S. and Bax, A. (1991) *J. Am. Chem. Soc.*, **113**, 5490–5492.

States, D.J., Haberkorn, R.A. and Ruben, D.J. (1982) *J. Magn. Reson.*, **48**, 286–292.

Takahashi, H., Odaka, A., Kawaminami, S., Matsunga, C., Kato, K., Shimada, I. and Arata, Y. (1991) *Biochemistry*, **30**, 6611–6619.

Takahashi, H., Suzuki, E., Shimada, I. and Arata, Y. (1992) *Biochemistry*, **31**, 2464–2468.

Wishart, D.S., Sykes, B.D. and Richards, F.M. (1991) *J. Mol. Biol.*, **222**, 311–333.

Wittekind, M., Gorlach, M., Friedrichs, M., Dreyfuss, G. and Mueller, L. (1992) *Biochemistry*, **31**, 6254–6265.

Wright, P.E., Dyson, H.J., Lerner, R.A., Riechman, L. and Tsang, P. (1990) *Biochem. Pharmacol.*, **40**, 83–88.

Zhu, G. and Bax, A. (1992) *J. Magn. Reson.*, **90**, 405.